This is the Pre-Published Version.

P. Sun, Y. Jia, X. Zhang, X. Huang (2021) *Fire Risk of Dripping Flame: Piloted Ignition and Soaking Effect*, **Fire Safety Journal**, 103360. https://doi.org/10.1016/j.firesaf.2021.103360

Fire Risk of Dripping Flame: Piloted Ignition and Soaking Effect

Peiyi Sun[1,2], Yifan Jia[1], Xiaoning Zhang[1], Xinyan Huang[1,*]

[1]*Research Centre for Fire Safety Engineering, Department of Building Services Engineering, The Hong Kong Polytechnic University, Kowloon, Hong Kong*

[2]*The Hong Kong Polytechnic University Shenzhen Research Institute, Shenzhen, China.*

*Corresponding to xy.huang@polyu.edu.hk

Abstract:

The dripping of thermoplastic fuels is a significant fire hazard, but the complex dripping-ignition process is still not fully understood. In this work, we investigate the ignition capability of continual polyethylene drips with the size of 2.6-4.6 mg and the frequency of 0.3-1 Hz. These flaming drips land on four groups of materials, cardstock papers (>0.1 mm), thin papers (≤0.1 mm), cotton, and porous mineral materials. For igniting cardstock papers, the minimum drip number decreases with the drip size and frequency, and the ignition time follows the piloted-ignition theory. The thin permeable paper and cotton are soaked by drips, so ignition only requires a small and fixed number of drips. The soaking effect also helps anchor the flame on drips absorbed by other porous mineral materials, showing a notable fire risk. Theoretical analysis of the ignition limit and delay time is proposed to identify the boundary between the piloted dripping ignition and the flame anchored on drip-soaked material. This research reveals different ignition mechanisms of dripping fire and helps understand the fire hazard regarding the transport and soaking effect of molten fuels.

Keywords: *Polyethylene drip; Ignition limit; Molten plastics; Porous fuel; Soaked material; Anchored flame.*

1. Introduction

Dripping fire is a special fire phenomenon that often happens on in fire accidents fueled by thermoplastics, such as fires in cable insulation, building façade, and plastic billboard (Fig. 1). For example, in the tragic event of the 1981 Stardust night club fire, Dublin, Ireland, the molten polymeric lining on the ceiling generated burning drips that ignited the PU seat-cushions, and finally, the intense fire burned out the entire building. In 2016, a large façade fire occurred at two residential towers in Ajman, Dubai, where the massive molten thermoplastic flowed downwards and fell along with other solid debris to accelerate the downward flame spread over the building cladding (Fig. 1a) [1]. Discrete drips with flame often take place in burning cables, although the fuel load on electric cables is small (Fig. 1b). Once heated in a fire, many thermoplastics, such as polyethylene (PE), polyethylene chloride (PVC), polypropylene (PP), and expanded polystyrene (EPS), can generate dripping flame [2–7]. These dripped plastics can flow like a liquid fuel [8–10] and form a pool fire (Fig. 1c). The dripping of thermoplastics could remotely ignite new fires, promote the fire spread [11,12], and lead to flashover, poses a big challenge for building fire safety [13].

Nomenclature

Symbols

A	area (mm^2)
c	geometry factor
c_p	specific heat (kJ/kg/K)
d	pore/fiber size (μm)
D	diameter (mm)
f	frequency (Hz)
g	gravity acceleration (m/s^2)
h	convection coefficient (W/m^2-K)
Δh	enthalpy (J/kg)
k	permeability
L	charactersitc length (m)
m	mass
$\dot{m}$	mass rate (mg/s)
M_{dr}	mass of one drip (mg)
n	repeat test number (-)
N	number of drips (-)
P	probability
$\dot{q}''$	heat flux (kW/m^2)
t	time (s)
T	temperature (°C)

Greeks

δ	thickness (mm)
ε	emissivity
η	heating efficiency
μ	viscosity
ρ	density (kg/m^3)
σ	Stefan–Boltzmann constant (W·m^{-2}·K^{-4})
τ	tortuosity
ϕ	porosity

Subscripts

b	bulk
crt	critical
dr	dripping
ig	ignition
L	molten PE layer
p	paper
py	pyrolysis
PE	polyethylene
s	solid
tot	total

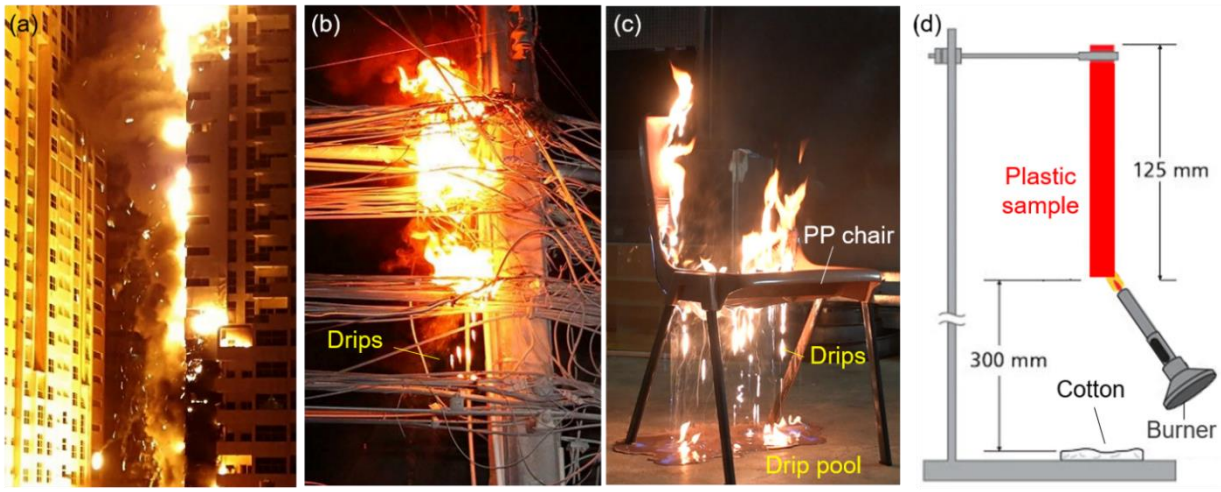

Fig. 1. Dripping fire phenomenon involved in (a) facade fire accidents [1], (b) wire fire cases [14], (c) compartment fire, and (d) UL 94 standard test [15].

The fire hazard of dripped thermoplastic pool fire has been investigated through different test setups in past researches [8,9,16], and particularly, the fast flow of molten PE shows a significant fire hazard [17–19]. In terms of the dripping flame, several standard tests consider the capacity of drip generation and the ignitibility of drips, such as the UL 94 material flammability test [20] (Fig. 1d) and the BS-EN-ISO 11925-2:2020 flame impingement test [21]. A number of studies used these standard tests to interpret the dripping characteristics of different thermoplastic materials. Wang *et al*. [2,22] examined the tendency of melting and dripping for multiple polymers through the UL 94 test. They found that the typical mass of drip was small, about 3.5 mg for polyethylene (PE) and 3-6 mg for polypropylene (PP) [23,24]. Kandola *et al*. [25] quantified the polymer degradation amid the melt dripping and measured the temperature of drips without a flame. Several numerical models are also established in simulating the melt dripping process in the UL 94 test [26]. The dripping mass and frequency have also been studied in wire fire tests [27–29] and numerical models [30].

Previously, we discovered that the flame attachment of drip was the necessary condition for dripping ignition [3]. The ignition of normal papers by continual drips followed the classical piloted ignition theory for the thermally thin fuel, that is, the difficulty of dripping ignition increases with the paper thickness. The dripping ignition time is proportional to the drip size and the square of dripping frequency [4]. Nevertheless, more insights are needed to reveal the underlying mechanisms in different types of dripping ignition. Especially, there is a complex interaction between the dripping fuel and the target material. The properties of target materials, such as chemical composition, thickness, density and porosity, also affect the dripping ignition process. When a large amount of drips land on the inert ground, a pool fire can be formed, indicating that the pre-landed melts are ignited by later drips. Overall, the traditional classification of thermally thin or thick fuel is not sufficient to explain the complex dripping ignition.

In this study, continual PE drips with the mass of 2.6-4.6 mg per drip and the dripping frequency of 0.3-1 Hz are produced. Four groups of target materials, (I) cardstock papers (>0.1 mm), (II) thin papers (≤0.1 mm), (III) cotton, and (IV) porous mineral materials, are selected to investigate different dripping-ignition behaviors. Experimental data are analyzed to improve the dripping-ignition theory. Finally, a new method is proposed to classify the dripping ignitability of target material, considering both the thickness and the permeability.

2. Experiment methods

2.1. Thermoplastic drips

The dripping generator was upgraded from our previous work [3,4], and the schematic is shown in Fig. 2. Three different drips were generated from a burning PE tube of 1-mm wall by inserting different stainless steel (SS) tube (Table 1), where the molten PE tube was heated by the flame while cooled by the metal tube. The drips fell as its gravity overcame its surface tension which decreases significantly with the temperature. The PE drip was heated by the flame above its pyrolysis point, so that strong bubbling and bursting could be observed [7], indicating that the drip was porous.

In general, PE tubes with a larger diameter and wall thickness were associated with larger drips. The dripping frequency (f_{dr}) ranged from 1 Hz to 1.8 Hz, and was inversely proportional to the dripping mass (M_{dr}) from 4.6 mg to 2.6 mg. That is, a larger drip had a smaller frequency. Previous work hypothesized that the intensity of dripping ignition was controlled by the dripping mass rate ($\dot{m}_{dr}$) [4], and was equally controlled by the dripping frequency (f_{dr}) and the drip size (M_{dr}) as

$$\dot{m}_{dr} = M_{dr} f_{dr} \quad (1)$$

However, it has not been verified under a wide range of dripping mass rate.

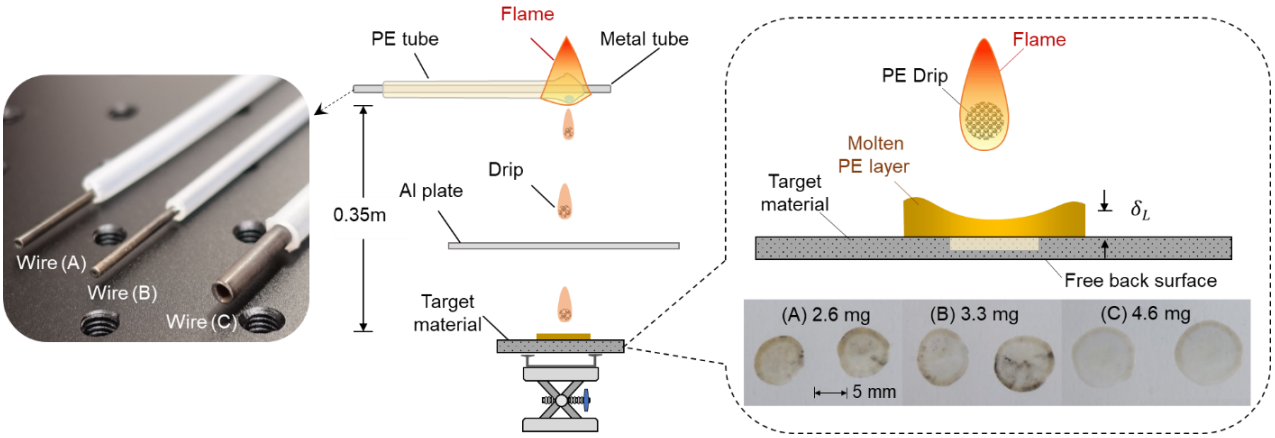

Fig. 2. Schematic diagrams of dripping ignition apparatus: wires to generate drips, where the PE drips self-compressed into a molted layer after reaching the target material.

Table 1. Characteristics of drip mass, frequency, diameter, and landing diameter, as well as the PE tube configuration, where the diameter of porous drip is calculated from the drip mass and density of 640 kg/m^3.

Drip Type	**A**	**B**	**C**
Drip diameter, d_{dr} (mm)	2.0	2.1	2.4
Mass of a drip, M_{dr} (mg)	2.6	3.3	4.6
Dripping frequency, f_{dr} (Hz)	1.8	1.4	1.0
Dripping mass rate, $\dot{m}_{dr}$ (mg/s)	4.7	4.6	4.6
Dripping heat flux, $\dot{q}''_{dr}$ (kW/m^2)	18±5	18±5	18±5
Heat of drip, q_{dr} (J)	1.0±0.3	1.3±0.4	1.8±0.5
Heat of dripping flame, q_f (J)	0.5±0.3	0.6±0.4	0.8±0.5
Molten layer diameter, d_L (mm)	6.7	7.7	9.6
PE tube inner diameter (mm)	3	2	4
SS tube wall thickness (mm)	0.2	0.7	0.4

To better control the dripping ignition intensity and vary the dripping mass rate, dripping mass and dripping frequency were controlled separately in two sets of tests.

(a) Fixing the dripping frequency at 1 Hz and changing the drip size from 2.6 mg to 4.6 mg, and

(b) Fixing the dripping mass at 4.6 mg and changing the dripping frequency from 1 Hz to 0.3 Hz.

As the dripping frequency was directly controlled by the burning PE tube, it could only be manually reduced by removing the unwanted drips before reaching the target materials. For example, if the original dripping frequency was 1 Hz, removing every other drip by a plate could create a new dripping frequency of 0.5 Hz.

2.2. Paper samples

Two white cardstock papers (Group I, δ_p > 0.1mm) and three thin papers (Group II, $\delta_p \leq$ 0.1mm) were selected as the target fuels (Fig. 3a). The size of the paper sample was 10 cm × 7 cm (i.e., A7), and the thickness was measured. More detailed parameters of all tested papers are listed in Table 2. As found in previous work [4], thick cardstock papers were not easily piloted, and many drips were needed for ignition. On the other hand, as the thickness decreases, paper becomes semi-transparent and permeable that can be soaked by landed drips. The thin filter paper is used in BS-EN-ISO 11925-2:2020 flame impingement test to indicate the dripping fire risk.

During the dripping ignition, temperatures on both the top and the bottom surfaces of paper were measured by two pairs of K-type thermocouples with 0.1 mm bead diameter (see more details in [4]). The temperature data were collected by a data logger every 0.1 s, which was much shorter than the time interval between two drips (about 1 s). Noted that all target materials in dripping ignition test were supported by a hollow mesh ring. Thus, the boundary condition at the back side of the sample was exposed to the cool ambient.

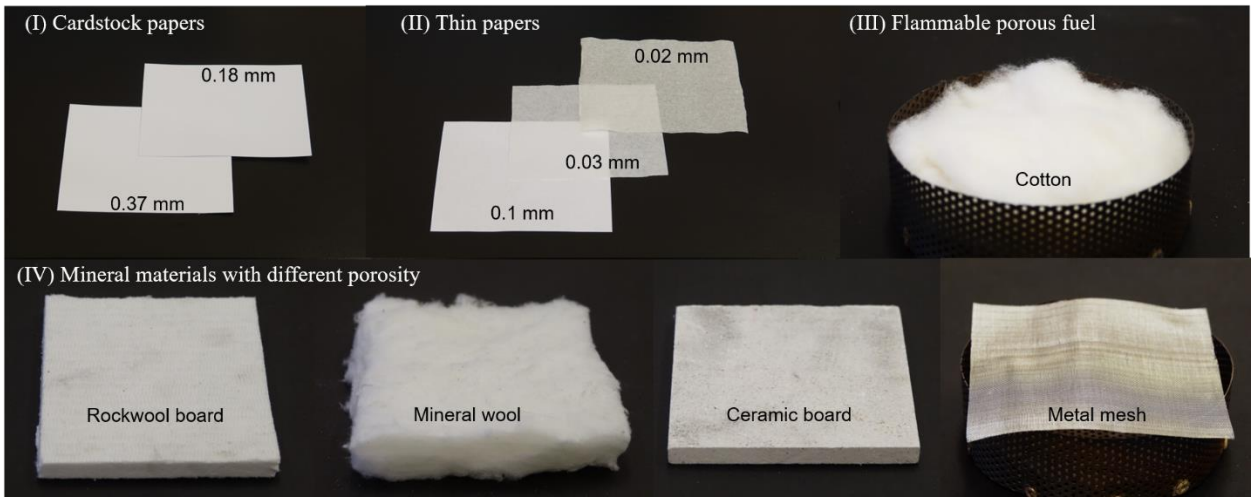

Fig. 3. Four group of target materials for dripping ignition, (I) two cardstock paper (> 0.1 mm), (II) three thin paper (≤ 0.1 mm), (III) cotton, and (IV) four porous mineral materials.

2.3. Other porous materials

To explore the how the soaking process influences the dripping ignition process, several porous materials were also tested. Their material properties are summarized and compared in Table 2. Cotton is a typical porous flammable fuel that is used in the UL 94 material flammability test [20] (Fig. 1d). Thus, a 30-mm thick cotton (Group III) was chosen and targeted by dripping flames (Fig. 3b). During the dripping ignition test, the cotton was the fuel because it was easily be ignited by a flame.

To further isolate the influence of flammability of the target material, four porous mineral materials (Group IV), Rockwool board, mineral wool, ceramic board, and metal mesh, were also "ignited" by dripping, that is, maintaining the dripping flame. All tested porous materials were thick, except that the metal mesh was one-layer and had a mesh size of 0.3 mm. The material porosity (ϕ) can be calculated from the material solid density (ρ_s) and the measured bulk density (ρ_b) [31], as

$$\phi = 1 - \frac{\rho_b}{\rho_s} \tag{2}$$

Table 2. Parameters of four groups of target materials including thickness (δ), area (A) mass (m), solid density (ρ_s), bulk density (ρ_b), porosity (ϕ), pore/fiber size (d), and permeability (k).

Fuel Group	Materials	δ (mm)	A (cm^2)	m (g)	ρ_s (kg/m^3)	ρ_b (kg/m^3)	ϕ (%)	d (μm)	k (m^2)
I	Cardstock paper 1	0.371		2.30		794	0.48		4.4×10^{-8}
	Cardstock paper 2	0.176		1.07		776	0.49		5.0×10^{-8}
	Thin print paper 1	0.103	10×7	0.62	1,550 [32]	769	0.50	10	5.2×10^{-8}
II	Thin print paper 2	0.034		0.11		419	0.73		5.3×10^{-7}
	1-layer tissue paper	0.022		0.06		329	0.78		1.1×10^{-6}
III	Cotton	30	86.6	4.5	1,500 [33]	17	0.98	20 [34]	2.5×10^{-4}
IV	Mineral wool	20	90.3	12.4	2,870 [35]	68	0.97	20 [36]	1.8×10^{-4}
	Rockwool board	10	10×10	30.7	2,870 [35]	307	0.89	20 [36]	6.8×10^{-6}
	Ceramic board	9	10×10	96.7	1,530 [37]	1,074	0.30	100	5.9×10^{-9}
	Metal Mesh	0.2	98.0	5.3	7,800 [38]	2,704	0.65	300	-

The permeability (k) can be estimated according to the Kozeny-Carman (KC) model [39], as

$$k = C_{KC}\frac{\phi^3}{(1-\phi)^2} \tag{3}$$

where $C_{KC} = cd^2/\tau \approx 1\times10^{-7}$ is an empirical parameter related to the geometry (c), tortuosity (τ), and fiber/pore size (d) of the porous media [39]. The calculated material porosity and permeability are listed in Table 2. The permeability of paper and ceramic board is at least four orders of magnitude smaller than cotton and wools, so that they are almost nonpermeable unless the thickness is very small ($\leq$ 0.1 mm).

3. Experimental results

Due to the complex dripping ignition process and the large experimental uncertainty, a statistical analysis method was also applied in this study [4,40]. For any given test condition, after many repeating tests, the dripping ignition probability was

$$P_{ig} = \frac{n_{ig}}{n_{tot}} \times 100\% \tag{4}$$

which represented the ratio of the number of ignition cases (n_{ig}) versus the total tests (n_{tot}). In the experiment, the observed successful "dripping ignition" included two types:

(1) the piloted ignition of the target fuel by hot drips and dripping flames, and

(2) the dripping flame is anchored on the drip-soaked material.

Note that for the inert target material, the observed ignition is actually the ignition of the pre-landed PE layer. During the ignition test, the fast contact between the drip, target material and flame, it is difficult to visually judge which type of dripping ignition occurs for thin papers and cotton. Thus, comparing different dripping sources and target materials, as well as comprehensive analysis is needed.

3.1. Dripping ignition of papers

Fig. 4 shows (a) the failed and (b) the successful dripping ignition process of the 0.18-mm thick cardstock paper (Group I), where and the dripping frequency is 1 Hz with a drip size of 4.6 mg. More detailed ignition process can be found in Supplemental Videos S1 and S2. As the number of drips increases from six to seven, eventually they can ignite the paper. Here, the dripping ignition limit is about seven drips. All drips were associated with a flame, because of a short dripping height, and continually landed at the same location on the paper. Once the hot drip impacted the paper, the bubbling ellipsoid droplet self-compressed into a thin layer. At the same time, all internal bubbles broke to generate a lot of pyrolysis gases, which were ignited by the following dripping flame. As a result, an intense explosion with a blue and ring-shape flame was observed (Fig. 4b and Video S2).

Note that the flame only lasted for about 100 ms, so that it could neither be maintained on the PE layer nor ignite the paper. It is mainly because the hot molten layer was cooled below its pyrolysis point by the cold paper, while the heating of dripping flame was insufficient. Meanwhile, the paper was heated by the hot drips and gradually charred and pyrolyzed (Fig. 4). As more drips continued to land, the areas of the molten layer and the charred paper expanded gradually, and finally, the ignition of paper was triggered (Fig. 4b). The charring of the paper was a necessary condition for the observed dripping ignition and burnout, which also suggested that the observed dripping ignition involves the pyrolysis gas of paper [4].

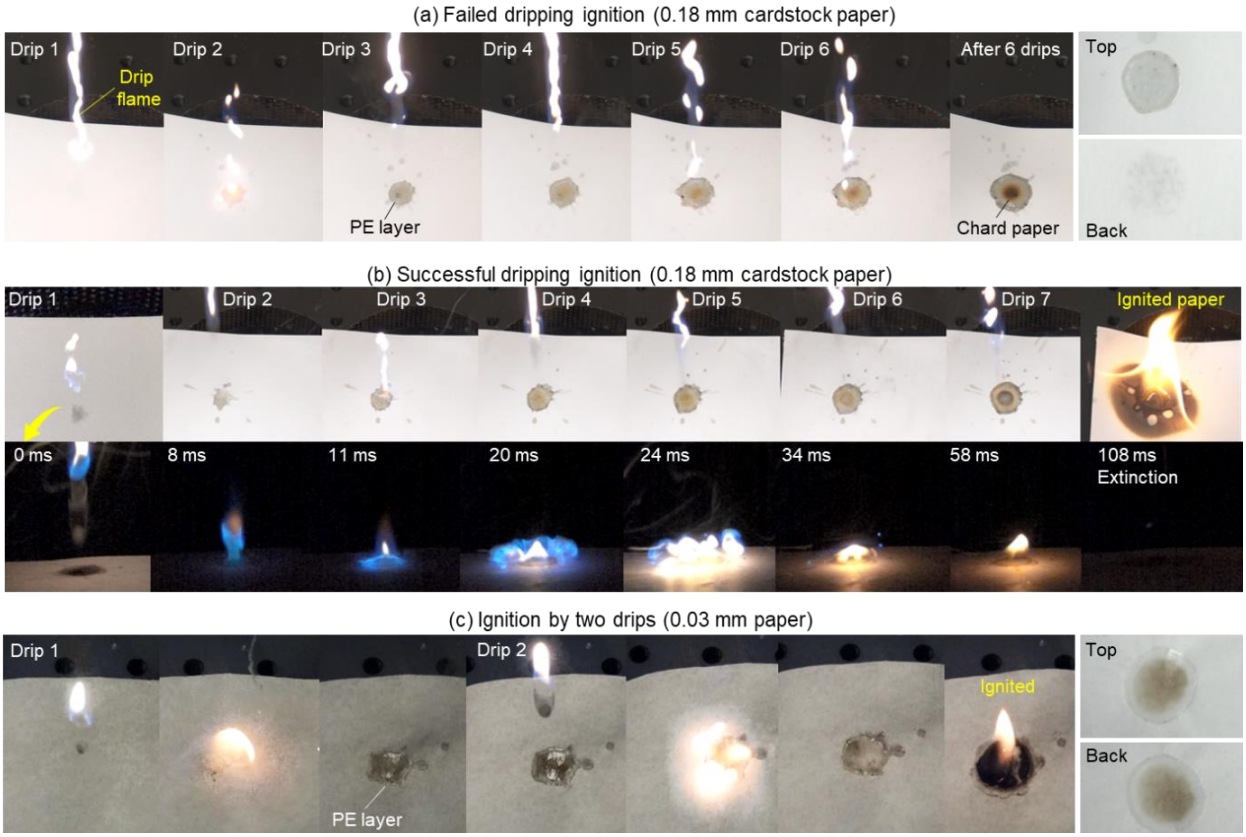

Fig. 4. Dripping ignition of paper with the drip size of 4.6 mg and frequency of 1 Hz (a) failed ignition by six drips (Video S1) and (b) ignition by seven drips of 0.18-mm cardstock paper and the drip landing process, lasted for less than 100 ms (Video S2), (c) ignition of 0.03-mm paper by two drips (Video S3).

On the other hand, very thin papers (thickness ≤ 0.1 mm) can be more easily ignited by a fewer number of drips. Fig. 4c shows the dripping ignition process for the 0.03-mm thin paper, where as few as two drips are sufficient for ignition (see Video S3). After the first drip landed, ignition did not occur, and like the thick cardstock paper, the landed drip also formed a molten layer above the paper surface. In contrast, part of the molten PE penetrated and soaked the permeable thin paper. Thus, the contour of the molten layer was clearly observed from the backside (Fig. 4c), different from the thick cardstock papers (Fig. 4a). Moreover, the cooling effect of thin paper is weaker, so that molten PE was only partially solidified. When the second drip landed, the dripping flame successfully anchored on the molten PE that was absorbed by the thin paper and quickly burned out the paper.

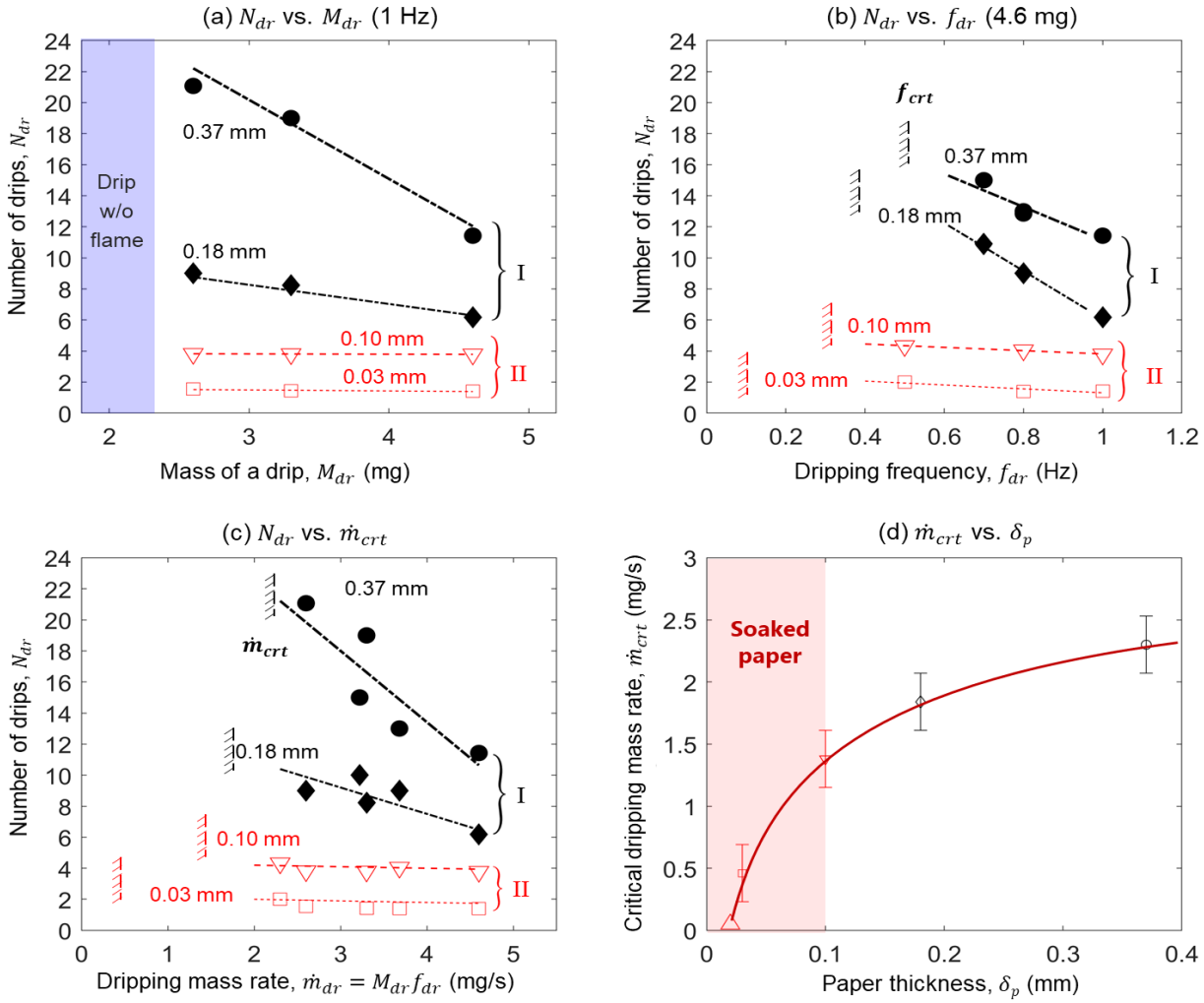

Fig. 5. The critical drip number (N_{dr}) for ignition at (a) fixed dripping frequency of 1 Hz and (b) fixed drip size of 4.6 mg, and (c) dripping mass rate, (d) the critical dripping mass rate versus with the paper thickness.

Fig. 5a-b summarizes the measured dripping ignition limit, that is, 50% ignition probability (P_{ig}), for two cardstock papers (solid symbols) and two thin papers (hollow symbols). The detailed ignition probability diagrams for all paper samples are summarized in Figs. A1 and A2. For the Test Set (a), the dripping frequency was fixed at 1 Hz, and the drip size varied from 2.6 mg to 4.6 mg. Essentially, two basic tendencies are observed.

For cardstock papers, the critical drip number for ignition decreases with the drip size. However, for thin papers, the critical drip number is almost constant and independent of the drip size. For example, about four drips can successfully ignite the 0.10-mm thin paper, no matter the drip is 2.6 mg or 4.6 mg. Noted that as the size of a drip decreases below 2.3 mg, these small dips can no longer carry with a flame after falling for 50 cm [3,41], so that the risk of dripping ignition becomes small.

A similar trend is also observed in the Test Set (b) in Fig. 5b, where the drip size is fixed to 4.6 mg, and the dripping frequency varies from 0.3 Hz to 1.0 Hz. The critical number of drips decreases with the dripping frequency for the cardstock paper, but for the thin paper, the required dripping number for ignition is almost a constant (Fig. 5b). Reducing the dripping frequency, the effective dripping heating decreases. Eventually, no matter how many drips have landed, ignition will not occur. For example, when the 0.18-mm paper was impacted by 4.6 mg drips, the ignition cannot happen when the frequency is lower than 0.4 Hz. Thus, a critical (or minimum) dripping frequency (f_{crt}) can be defined for the dripping ignition. With the thickness of the paper reduces, the critical dripping frequency decreases.

These two sets of experiments prove that the required drip number (N_{dr}) to ignite the cardstock paper is inversely proportional to both the drip size (M_{dr}) and frequency (f_{dr}). Fig. 5c further plots the required drip number (N_{dr}) vs. the dripping mass rate ($\dot{m}_{dr}$). Thus, we can conclude that the effective heat flux ($\dot{q}''_{dr}$) of the dripping ignition is controlled by the dripping mass rate as

$$\dot{q}''_{dr} \propto \dot{m}_{dr} = M_{dr} f_{dr} \qquad (N \geq 2) \qquad (5a)$$

Noted that above heat flux quantification is only appliable for multi-drips ignition occasions, as there is no dripping frequency for the one drip ignition case. On the other hand, Fig. 5a-c also implies that the dripping ignition of thin paper is not fully controlled by the dripping mass rate (or heat flux), because the effect of soaking becomes important. Similarly, the minimum dripping mass rate ($\dot{m}_{crt}$) or the critical dripping intensity was found in Fig. 5c and replotted in Fig. 5d. As expected, a smaller $\dot{m}_{crt}$ is needed for a thinner paper. Eventually, this critical dripping mass rate drops to zero for the 0.02-mm tissue paper or not exist anymore, because only one drip is sufficient for ignition.

3.2. Flame anchored on soaked materials

Fig. 6a shows a successful dripping ignition process of the cotton sample by one drip (see Video S4). In all repeating experiments, one drip could easily ignite the cotton, as long as the drip carried a flame. Once the PE droplet got in contact with the cotton (set as 0 ms), it was immediately absorbed by the cotton fibers like a soaked wick. Just after 13 ms, the associated dripping flame piloted the soaked cotton fiber. Such a yellow flame quickly ignited the nearby fibers, spread over the entire cotton surface within 0.5 s, and burnt out the fuel in less than 2 s. After the extinction of the flame, the cotton was completely charred, and the smoldering fire lasted for more than 5 min [42].

Fig. 6b shows the successful "ignition" of mineral wool by one drip (see Video S5). Compared with the cotton fiber, the interaction between the dripping flame and mineral wool was less intensive, mainly because the mineral wool was not flammable to intensify the fire. Nevertheless, the flame could still anchor on the soaked wool for more than 15 s until the PE drip was burnt out. Such a burning time is not only 100 times longer than the unstable drip flame observed on the cardstock paper (see Fig. 4b), but also similar to calculated burnout time (about 10 s) of a PE droplet [7]. For the consolidated Rockwool board (Fig. 6c and Video S6), it took about three

drips for the dripping flame to anchor. The flames of first two drips were quickly extinguished after landing, that is, lasted for less than 0.5s. After the third drip, the flame was anchored and lasted for around 5 s, although it was relatively weak. Therefore, the anchored flame on the drip-soaked porous media was observed as a different type of "dripping ignition."

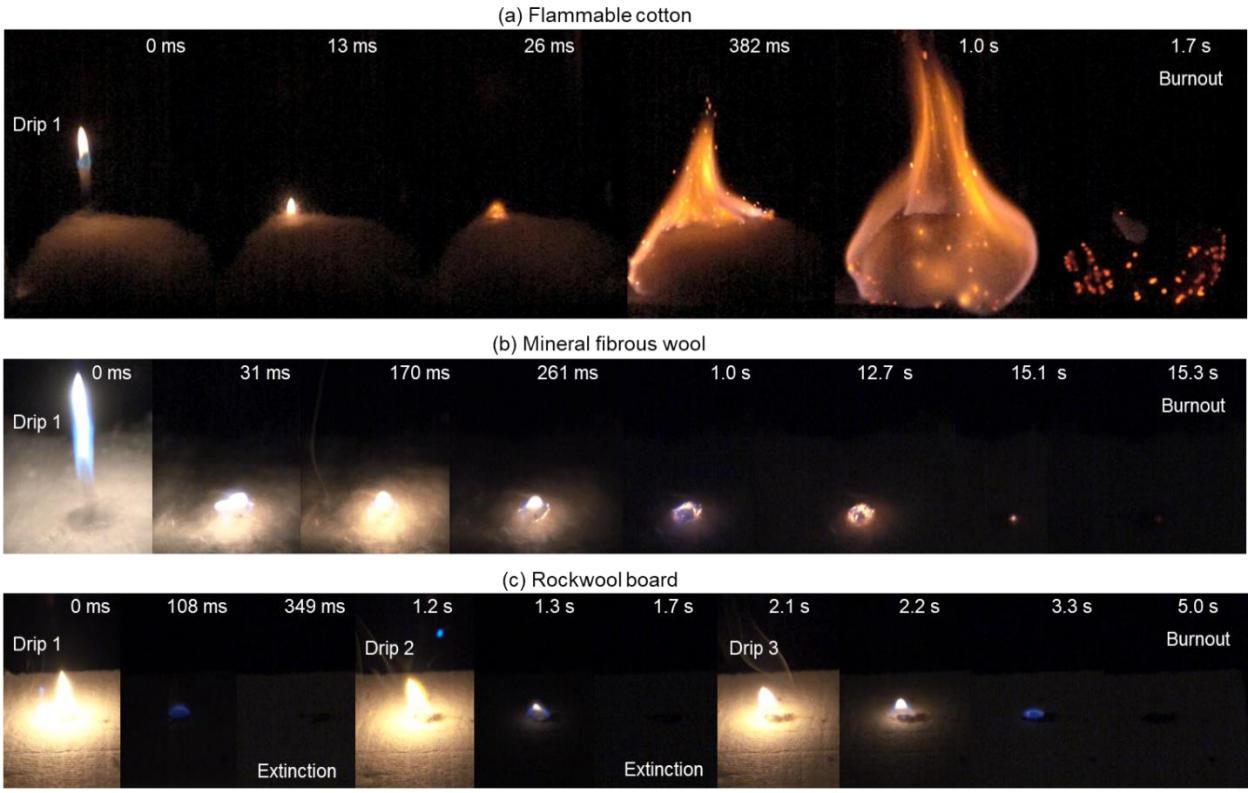

Fig. 6. Snapshots of the landing process of PE drips and flame on different porous materials, (a) cotton (Video S4), (b) mineral wool (Video S5), and (c) Rockwool board (Video S6), where the drip size is 4.6 mg.

For the less-porous ceramic board, it cannot support the dripping flame under the maximum dripping mass rate of 4.6 mg/s (see Video S7). For the metal mesh, at least ten drips are needed to anchor the dripping flame, because it has a large cooling effect and is too thin and permeable to hold all landed drips (see Video S8). As the material permeability decreases, the soaking process becomes harder and slower; and the increased material bulk density and thermal inertia weaken drips' heating effect. Both reasons make the dripping flame more difficult to anchor on the target material.

Fig. 7 summarizes the minimum drip number for igniting all four groups of materials under (a) varied drip size (M_{dr}) and (b) varied dripping mass rate ($\dot{m}_{dr}$). Fewer than five drips are needed to anchor the flame on four drip-soaked permeable materials, i.e., thin paper, cotton, mineral wool, and Rockwool board. The required drip number is much smaller than that for igniting a cardstock paper. More importantly, the required number of drips is insensitive to the drip size (M_{dr}) or the dripping mass rate ($\dot{m}_{dr}$). This similarity further confirms that the observed dripping "ignition" on soaked materials is different from the dripping piloted ignition of thick cardstock papers.

For metal mesh (Fig. 7a), the limiting dripping ignition condition is special and different from all other materials, where the required number of drips increases with the drip size. Unlike the homogenous porous material, the discrete metal mesh has a unique one-layer structure that can only hold a limited amount of drips. Thus, part of landed drips pass through the metal mesh (see Video S8), especially for larger drips that have a larger momentum. In contrast, for smaller drips, most could remain on the mesh after landing to soak and heat the mesh; thus, the smaller drip only needs a smaller number of drips to anchor the flame.

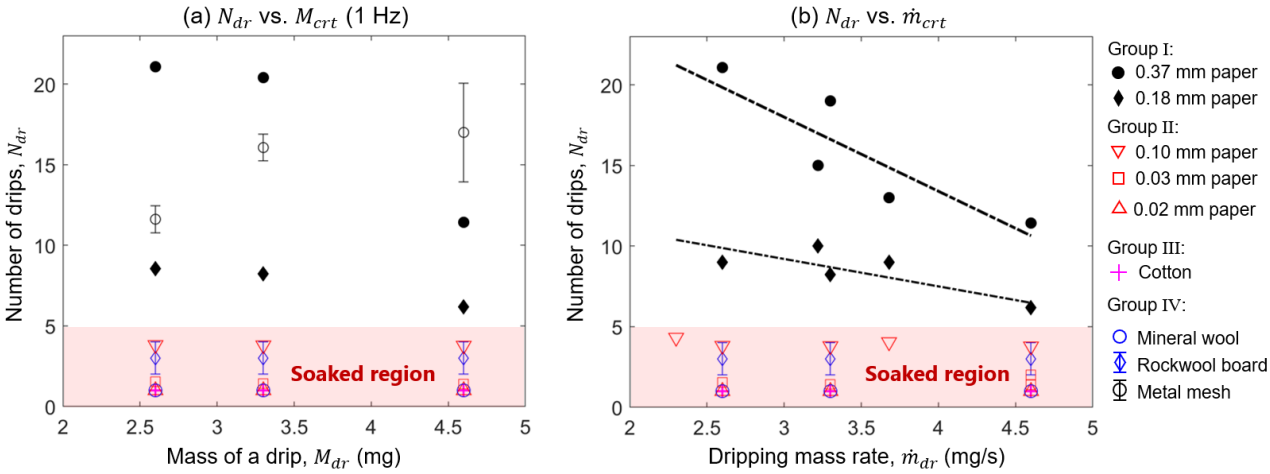

Fig. 7. The critical number of drips to trigger an ignition vs (a) the drip size under the constant dripping frequency (1 Hz), and (b) the dripping mass rate for all four groups of target materials.

In short, the porous and permeable materials, regardless they are flammable or mineral, can be soaked by molten drips to help anchor the dripping flame, driven by both the capillary action and surface tension. The principle is similar to the candle flame. That is, it is difficult to ignite the wax directly because it has a high flashpoint (240-260 °C [43]); however, it is easy to ignite the wick that is soaked by the molten wax. Therefore, we can conclude that the ease of dripping ignition increases, as both the flammability and soaking capability of target material increase. Moreover, compared with common non-porous flammable materials (e.g. thick cardstock papers and plastics), porous soaked materials could be much easier to achieve the dripping ignition or anchor the dripping flame, showing a greater dripping fire risk and hazard.

4. Discussion

4.1. Heat flux of dripping ignition

As first revealed in our previous work [4], the dripping ignition of cardstock paper is the piloted ignition, where the dripping flame is the pilot sources, and both the hot drip and dripping flame are the heat sources, i.e., the Type (1) dripping ignition. To determine the critical ignition conditions, the equivalent heat flux should be quantified. The principle of this measurement is similar to the thin-skin heat flux gauge [44]. Thus, the dripping heat flux can be calculated from the temperature evolution of paper (T_p) and the lumped heat transfer model [43], as

$$\dot{q}''_{dr} = \rho_p c_p \delta_p \frac{dT_p}{dt} + h\left(T_p - T_a\right) + \varepsilon_p \sigma\left(T_p^4 - T_a^4\right) \quad (6)$$

where $\rho_p = 930$ kg/m3, $c_p = 1.34$ kJ/kg-K [45], $\varepsilon_p = 0.95$, and δ_p are the density, specific heat, emissivity, and thickness of paper, respectively; $h \approx 10$ W/m^2-K is the convective coefficient [46]; $T_a = 295$ K is the room temperature; and $\sigma = 5.67 \times 10^{-8}$ W·m^{-2}·K^{-4} is the Stefan–Boltzmann constant.

The average paper temperature below the molten PE layer was measured by two thermocouples. Fig. 8 shows some representative temperature of on the paper top and back surfaces, as well as the calculated dripping heat flux ($\dot{q}''_{dr}$) under different dripping fire impacts. As expected, the top-surface temperature fluctuates significantly, and each peak denotes the landing of a drip. For thick cardstock (> 0.1 mm in Fig. 8a-b), the back-surface temperature has negligible fluctuation, because the molten PE cannot easily penetrate to the back (also see Fig. 4). On the other hand, for the thin paper (≤ 0.1 mm in Fig. 8c), the back-surface temperature fluctuates along with the top-surface temperature. Such a phenomenon further reveals that the thin paper is soaked and heated in-depth by the molten PE.

The calculated instantaneous dripping heat flux can become negative for thick cardstock papers (Fig. 8a-b), because at the interval between drips, the paper is cooled by the environment. While for the soaked thin paper (Fig. 8c), the instantaneous dripping heat flux is always positive, because it is continuously soaked and heated by the penetrated hot molten PE. After about 15 drips for 0.37-mm paper (Fig. 8b) and 5 drips for the 0.10-mm paper (Fig. 8c), the average temperature of paper reaches a plateau, and the equivalent dripping heat flux also approaches a constant. Further increasing the number of drips, both the average temperature and heat flux gradually decrease, as the thickness of the molten PE layer or the thermal inertia of target material increases.

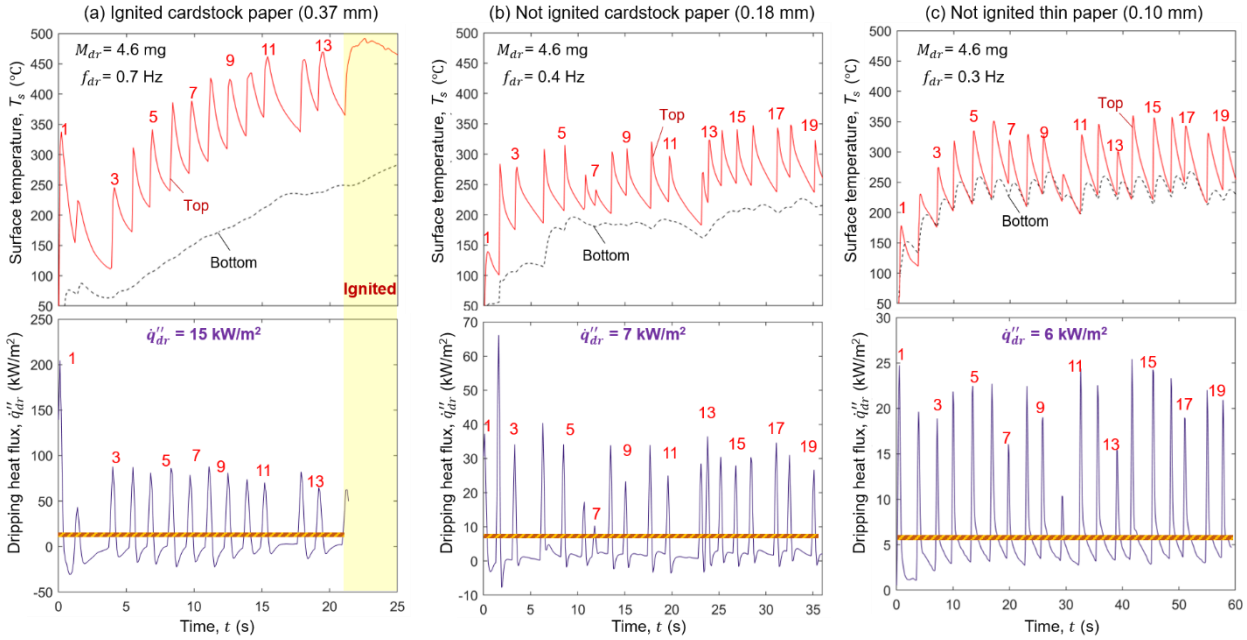

Fig. 8. Paper surface temperatures and dripping heat flux, (a) 0.37-mm cardstock ignited under the dripping frequency of 0.7 Hz, (b) 0.18-mm cardstock not ignited under the dripping frequency of 0.4 Hz, and (c) 0.10-mm thin paper not ignited under the dripping frequency of 0.3 Hz, where the drip size is fixed to 4.6 mg.

Based on the heat transfer analysis, we previously proposed an analytical expression for the effective dripping heat flux ($\dot{q}''_{dr}$) [4] as

$$\dot{q}''_{dr} = \frac{1}{\bar{A}}\left(q_{dr} + q_f\right) f_{dr} = \frac{1}{\bar{A}}\left(\Delta h_{dr} + \Delta h_f\right)\dot{m}_{dr} \qquad (5b)$$

where $\bar{A} = 1.5$ cm^2 is the measured effective heating area of the molten layer; $\Delta h_{dr} = c_p\left(T_{dr} - T_{py}\right)$ and Δh_f is the effective heat per drip mass from the hot drip and dripping flame, respectively. T_{dr} is the temperature of PE drip (about 450 °C), and T_{py} is the pyrolysis temperature of target fuel (250-350 °C). This hypothesis, that it, the dripping heat flux is proportional to the dripping mass rate, has not been verified until this work when the dripping frequency and mass rate are controlled and varied.

Fig. 9 shows the measured dripping heat flux varying with (a) the dripping frequency f_{dr} and (b) the dripping mass rate $\dot{m}_{dr}$. Clearly, a good linear correlation can be observed; thus, proving the hypothesis of Eq. (5). Then, the dripping ignition heat from hot drip and dripping flame can be estimated

$$\Delta h_{dr} \approx 0.40 \pm 0.10 \text{ J/mg}, \quad \Delta h_f \approx 0.10 \pm 0.05 \text{ J/mg}, \qquad (7)$$

Thus, the hot drip contributes to the heating of the target fuel more than the flame of drip.

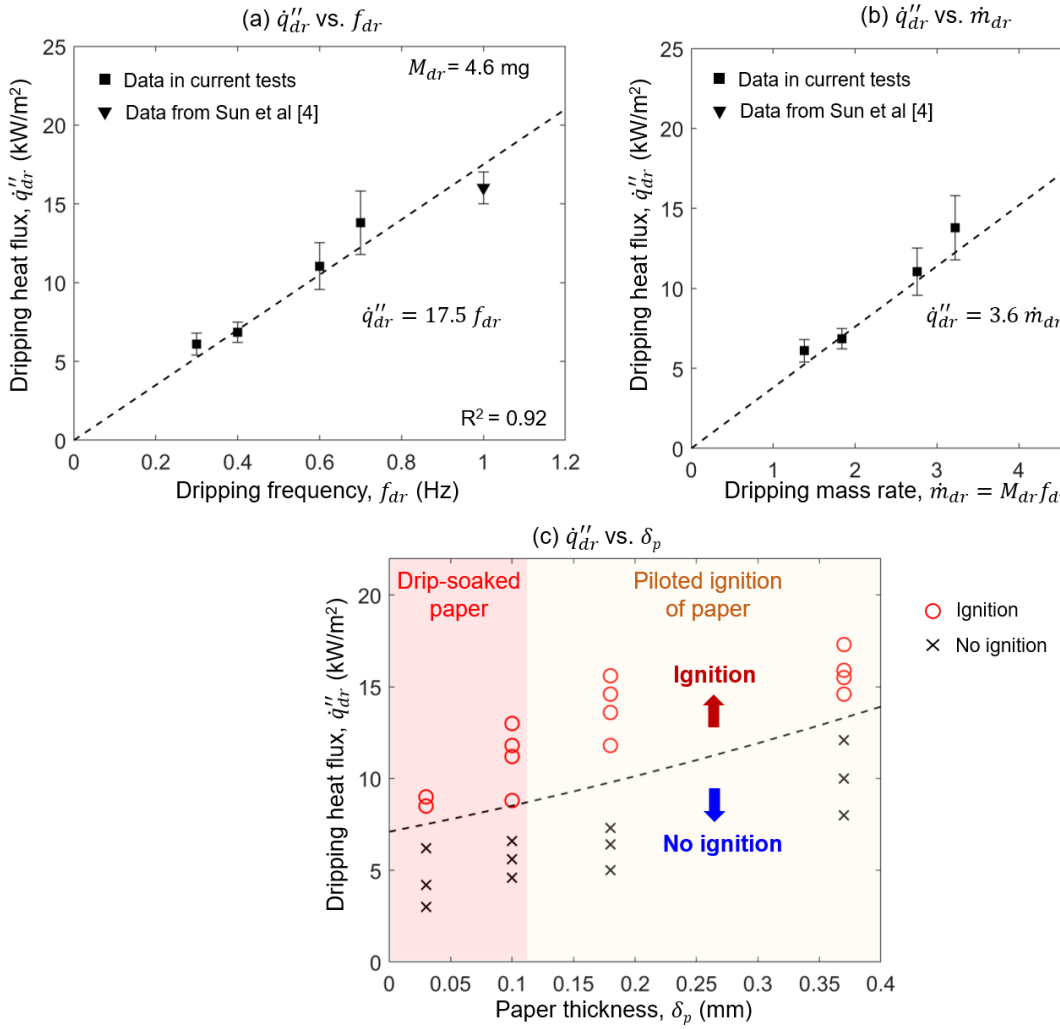

Fig. 9. The effective dripping heat flux as a function of (a) dripping frequency f_{dr} and (b) the dripping mass rate $\dot{m}_{dr}$, and (c) the critical dripping-ignition heat flux $\dot{q}''_{dr}$ vs the paper thickness δ_p.

As seen from Eq. (5) and Fig. 9a-b, increasing the drip size and frequency raises the dripping heat flux and promotes the piloted ignition. It is because an intensive and frequent dripping can overcome the environmental cooling and heat the paper above its pyrolysis point (250-300 °C in Fig. 8). If the dripping frequency decreases, the effective dripping heat flux also decreases, and eventually, the dripping ignition becomes impossible. For example, as f_{dr} decreases from 0.7 Hz (Fig. 8a) to 0.3 Hz (Fig. 8c), $\dot{q}''_{dr}$ decreases from 15 kW/m^2 to 6 kW/m^2. Then, the top-surface temperature barely exceeds 300 °C even after 35 drips, so there will not be a dripping ignition.

In practice, if the target fuel cannot get piloted after 20 drips, the chance of ignition becomes slim. Thus, there is also a minimum (or critical) heat flux for dripping ignition ($\dot{q}''_{crt}$), like all other piloted-ignition processes. Fig. 9c summarizes the effective dripping heat flux for ignition and no-ignition cases, where the critical dripping heat flux is determined for papers of different thicknesses. For thin papers, the minimum heat flux for ignition can be as low as 8 kW/m^2, which is much lower than 12-14 kW/m^2 measured by the cone calorimeter. This observation also implies that if the paper thickness is smaller than 0.1 mm, the classical piloted ignition theory becomes inappropriate, and the effect of drip soaking becomes dominant.

4.2. Piloted ignition vs soaking effect

To further identify the boundary between (1) the piloted dripping ignition of target fuel and (2) the flame anchored on the drip-soaked material, the dripping ignition time of paper is further analyzed. Previously, we found that the dripping ignition time (t_{ig}) of cardstock papers follows the classical piloted ignition theory of the thermally thin fuel [4], as

$$t_{ig} \propto \frac{\delta}{\dot{q}''_{dr} f_{dr}} \propto \frac{\delta}{\dot{m}_{dr} f_{dr}} = \frac{\delta}{M_{dr} f_{dr}^2} \qquad \text{(piloted ignition)} \qquad (8a)$$

That is, the dripping ignition delay is proportional to the paper thickness (δ), while inversely proportional to the drip size (M_{dr}) and the square of dripping frequency (f_{dr}^2). Fig. 10a shows that for thick cardstock papers, Eq. (8a) successfully explain the measured dripping ignition time.

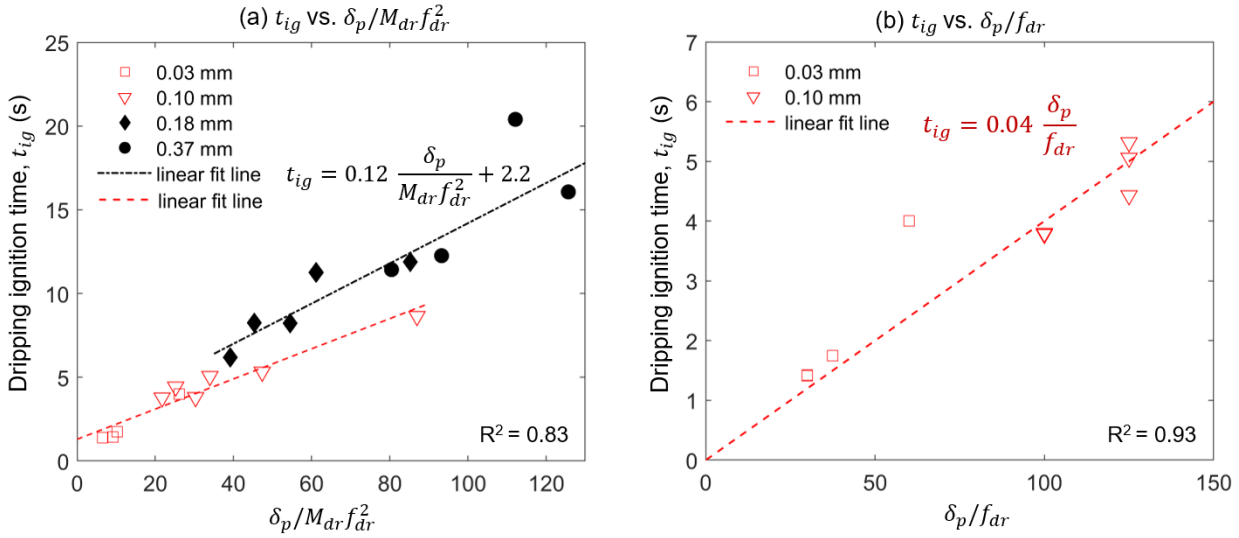

Fig. 10. The dripping ignition time for paper with different thickness following the function of (a) $\delta/M_{dr}f_{dr}^2$ and (b) δ/f_{dr}, where 0.02-mm paper is not shown because it can be ignited by one drip (no frequency).

However, as the paper becomes thinner, it is easier to be soaked by hot drips, which can be understood from the reducing permeability with an increasing paper thickness (Table. 2). Then, the observed dripping ignition becomes the dripping flame anchored on the drip-soaked paper, and such an ignition process is much easier and faster. In addition, the previous correlation of ignition time for thin paper has a different trend with the cardstock papers in Fig. 10a. Therefore, the ignition time no longer follows the classical piloted ignition theory (see Fig. 10a). Instead, it is independent of the dripping flux as

$$t_{ig} \propto \frac{\delta}{f_{dr}} \qquad \text{(flame on soaked paper)} \qquad (8b)$$

which is proportional to the paper thickness and inversely proportional to the dripping frequency. Such correlation is well verified by the experimental data in Fig. 10b.

Based on the analysis above, we can further quantify the required drip number (N_{ig}) for the anchored flame and extend to other permeable materials that can be soaked by hot drips, as

$$N_{ig} = t_{ig} f_{dr} \propto \begin{cases} \dfrac{\delta}{\dot{m}_{dr}} & \text{(piloted ignition)} \\ \delta & \text{(soaked flat surface)} \\ d & \text{(soaked porous media)} \end{cases} \qquad (9)$$

where d is the diameter of pore or fiber of the soaked porous media. Fig. 11a shows the required number of drips (N_{dr}) for the dripping ignition versus the characteristic size of the target material. A clear linear correlation is found for the soaked thin papers. However, the region of thick cardstock papers is well below the limit, because it is controlled by the dripping heat flux.

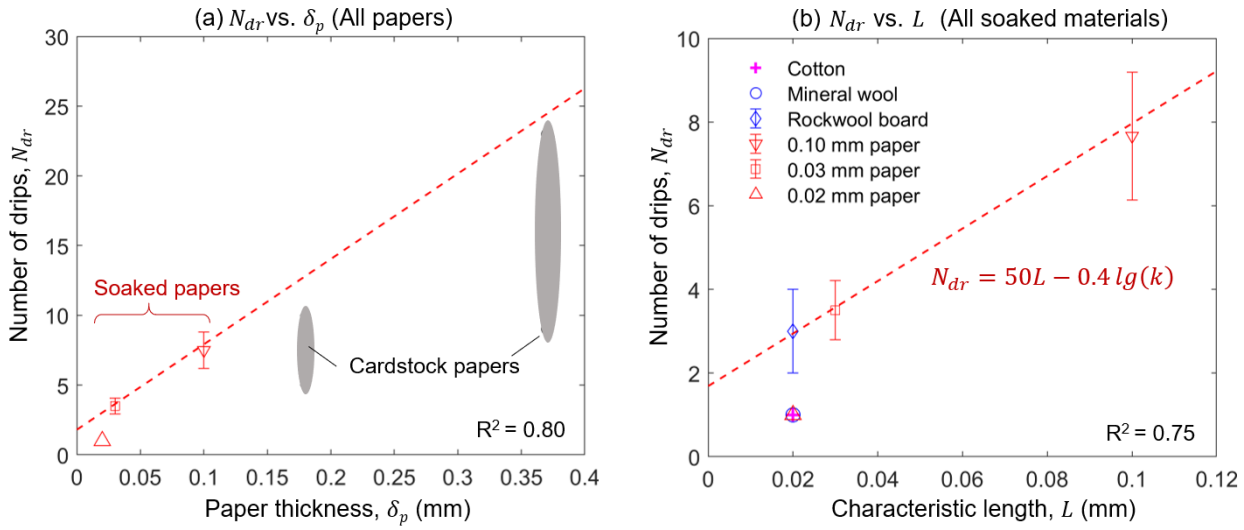

Fig. 11. The required number of drips (N_{dr}) for the dripping ignition versus (a) the thickness of paper, and (b) the characteristic length for all soaked materials.

Fig. 11b further tested Eq. (9) with all other soaked materials, where the characteristic length includes thickness for papers and diameter of pore or fiber. Clearly, a good linear correlation can explain most of the data,

which considers both the structural size (L) and permeability (k) of the soaked material. The structural size plays the dominant role, while the permeability becomes important, only if the material becomes difficult to penetrate.

Based on the experimental data and theoretical analysis above, Fig. 12 illustrates the interaction between two types of observed dripping ignition, namely, (1) the piloted dripping ignition of the target fuel and (2) the dripping flame anchored on the drip-soaked material. In general, the required drip number (or mass) to trigger either type of dripping ignition will vary with the dripping mass rate (or heat flux) and the characteristics of target material (structural size and permeability). Following the classic piloted ignition theory, to ignite a thick and nonpermeable fuel, the required drip mass decreases with the increasing dripping mass rate. As the thickness of the fuel increases, more drips are needed to heat the fuel. Moreover, the threshold of piloted dripping ignition has a minimum dripping heat flux, which is reflected by the minimum dripping mass rate ($\dot{m}_{crt}$).

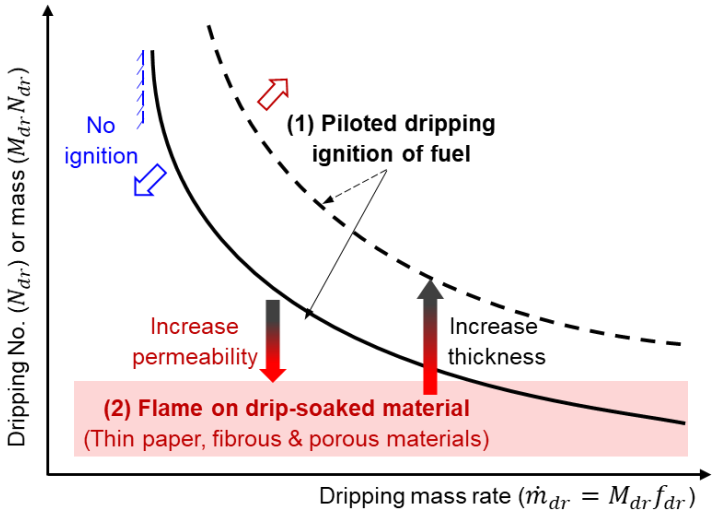

Fig. 12. Regions for two types of observed dripping ignition (1) the piloted dripping ignition of fuel and (2) the flame on the drip-soaked material, as well as key influence factors.

With the decrease of material thickness or the increase of material permeability, molten thermoplastic drips will start to soak the fuel. These drip-soaked materials could be mineral, as long as they can absorb the drip, so that they only need a small number of drips to anchor the flame. Moreover, the dripping mass rate (or heat flux) becomes less important, because the observed "ignition" is not a heating process, but a soaking process. Then, it will require a minimum amount of molten drips to sufficiently penetrate and soak the target material (see the red region in Fig. 12). As the material becomes more permeable, the soaking process of landed molten drips becomes easier. Then, only a smaller amount of drips is needed to anchor the dripping flame, so that the risk and hazard of dripping fire increases significantly.

5. Conclusions

A series of laboratory-scale dripping ignition experiments are conducted on four groups of materials: (I) cardstock papers, (II) thin papers, (III) cotton, and (IV) porous mineral materials using thermoplastic drips with specific dripping frequencies (0.3-1 Hz) and drip size (2.6-4.6 mg) separately. Two types of dripping "ignition" were identified and investigated, (1) the piloted dripping ignition of target fuels, and (2) the flame anchored on the drip-soaked material. For the thick cardstock paper, the critical dripping number decreases with the effective

dripping heat flux, following the classic piloted ignition theory. The dripping heat flux is controlled by the dripping mass rate (the product of the drip size and frequency), and there is a minimum dripping mass rate for ignition. The effective heat of hot drip and dripping flame for ignition is 0.4 ± 0.10 J/mg and 0.1 ± 0.05 J/mg per mass of drip, respectively.

As the target material becomes thinner and more permeable (e.g., thin paper, cotton, and mineral wool), a small and fixed number of drips are needed to soak the material and anchor the dripping flame, regardless the material flammability. Thus, the observed "ignition" is a soaking process rather than a heating process, which is almost independent of the dripping intensity or heat flux. As the material becomes more permeable, the soaking process of drips becomes easier, amplifying the dripping fire hazard. This study reveals different types and mechanisms of dripping ignition and helps understand the fire hazard of fuel transport and interaction.

Acknowledgments

This research is supported by the National Natural Science Foundation of China (NSFC) No. 51876183.

References

[1] AFP. Fire engulfs UAE residential towers. Yahoo News 2016.

[2] Wang Y, Jow J, Su K, Zhang J. Dripping behavior of burning polymers under UL94 vertical test conditions. Journal of Fire Sciences 2012;30:477–501. doi:10.1177/0734904112446125.

[3] Huang X. Critical Drip Size and Blue Flame Shedding of Dripping Ignition in Fire. Scientific Reports 2018;8:16528. doi:10.1038/s41598-018-34620-3.

[4] Sun P, Lin S, Huang X. Ignition of thin fuel by thermoplastic drips: An experimental study for the dripping ignition theory. Fire Safety Journal 2020;115:103006. doi:10.1016/j.firesaf.2020.103006.

[5] Wang S, Zhang Y, Huang X. Hot Particle Ignition of EPS Foam: Hollow Particles, Auto-ignition, and Fire Point. Fire Safety Journal (under Review) 2020.

[6] Hurley MJ, Gottuk DT, Jr. JRH, Harada K, Kuligowski ED, Puchovsky M, et al., editors. SFPE Handbook of Fire Protection Engineering, Springer; 2015.

[7] Sun P, Wu C, Zhu F, Wang S, Huang X. Microgravity combustion of polyethylene droplet in drop tower. Combustion and Flame 2020;222:18–26. doi:10.1016/j.combustflame.2020.08.032.

[8] Babrauskas V, Wickström UG. Thermoplastic pool compartment fires. Combustion and Flame 1979;34:195–202. doi:10.1016/0010-2180(79)90092-0.

[9] Zhang J, Shields TJ, Silcock GWH. Effect of melting behaviour on upward flame spread of thermoplastics. Fire and Materials 1997;21:1–6. doi:10.1002/(sici)1099-1018(199701)21:1<1::aid-fam583>3.3.co;2-g.

[10] Xie Q, Zhang H, Xu L. Large-scale experimental study on the effects of flooring materials on combustion behavior of thermoplastics. Journal of Macromolecular Science, Part A: Pure and Applied Chemistry 2008;45:529–33. doi:10.1080/10601320802100556.

[11] Williams FA. Mechanisms of fire spread. Symposium (International) on Combustion 1977;16:1281–94. doi:10.1016/S0082-0784(77)80415-3.

[12] Jiang Y, Zhai C, Shi L, Liu X, Gong J. Assessment of melting and dripping effect on ignition of vertically discrete polypropylene and polyethylene slabs. Journal of Thermal Analysis and

Calorimetry 2020. doi:10.1007/s10973-020-09575-1.

[13] Ohlemiller T, Shields J. Aspects of the fire behavior of thermoplastic materials. NIST Technical Note, 2008.

[14] Pigeon Pecks Through Power Cables And Sparks Chaos. Bangkok Extra n.d.

[15] Advanced Optical Plastics Materials for LED Lighting Applications by Styron LLC. LED Professional 2016.

[16] Wang X, Cheng X, Li L, Lo S, Zhang H. Effect of ignition condition on typical polymer's melt flow flammability. Journal of Hazardous Materials 2011;190:766–71. doi:10.1016/j.jhazmat.2011.03.108.

[17] Xie Q, Zhang H, Ye R. Experimental study on melting and flowing behavior of thermoplastics combustion based on a new setup with a T-shape trough. Journal of Hazardous Materials 2009;166:1321–5. doi:10.1016/j.jhazmat.2008.12.057.

[18] Ma X, Tu R, Xie Q, Jiang Y, Zhao Y, Wang N. Experimental study on the burning behaviors of three typical thermoplastic materials liquid pool fire with different mass feeding rates. Journal of Thermal Analysis and Calorimetry 2016;123:329–37. doi:10.1007/s10973-015-4898-0.

[19] Xie Q, Tu R, Wang N, Ma X, Jiang X. Experimental study on flowing burning behaviors of a pool fire with dripping of melted thermoplastics. Journal of Hazardous Materials 2014;267:48–54. doi:10.1016/j.jhazmat.2013.12.033.

[20] UL. Standard for Tests for Flammability of Plastic Materials for Parts in Devices and Appliances. UL 94 2013.

[21] BSI. BSI Standards Publication Reaction to fire tests – Ignitability of products subjected to direct impingement of flame. 2020.

[22] Wang Y, Zhang J. Thermal stabilities of drops of burning thermoplastics under the UL 94 vertical test conditions. Journal of Hazardous Materials 2013;246–247:103–9. doi:10.1016/j.jhazmat.2012.12.020.

[23] Kandola BK, Price D, Milnes GJ, Da Silva A, Gao F, Nigmatullin R. Characterization of melt dripping behavior of flame retarded polypropylene nanocomposites. ACS Symposium Series 2012;1118:311–25. doi:10.1021/bk-2012-1118.ch021.

[24] Joseph P, Tretsiakova-McNally S. Melt-flow behaviours of thermoplastic materials under fire conditions: Recent experimental studies and some theoretical approaches. Materials 2015;8:8793–803. doi:10.3390/ma8125492.

[25] Kandola BK, Ndiaye M, Price D. Quantification of polymer degradation during melt dripping of thermoplastic polymers. Polymer Degradation and Stability 2014;106:16–25. doi:10.1016/j.polymdegradstab.2013.12.020.

[26] Kempel F, Schartel B, Marti JM, Butler KM, Ross R, Idelsohn SR, et al. Modelling the vertical UL 94 test: competition and collaboration between melt dripping, gasification and combustion. Fire Mateiral 2015;39:570–84. doi:10.1002/fam.2257.

[27] Kobayashi Y, Huang X, Nakaya S, Tsue M, Fernandez-Pello C. Flame spread over horizontal and vertical wires: The role of dripping and core. Fire Safety Journal 2017;91:112–22.

doi:10.1016/j.firesaf.2017.03.047.

[28] Fang J, Zhang Y, Huang X, Xue Y, Wang J, Zhao S, et al. Dripping and Fire Extinction Limits of Thin Wire: Effect of Pressure and Oxygen. Combustion Science and Technology 2021;193:437–52. doi:10.1080/00102202.2019.1658578.

[29] Lim SJ, Kim M, Park J, Fujita O, Chung S. Flame spread over electrical wire with AC electric fields: Internal circulation, fuel vapor-jet, spread rate acceleration, and molten insulator dripping. Combustion and Flame 2015;162:1167–75. doi:10.1016/j.combustflame.2014.10.009.

[30] Kim Y, Hossain A, Nakamura Y. Numerical modeling of melting and dripping process of polymeric material subjected to moving heat flux: Prediction of drop time. Proceedings of the Combustion Institute 2015;35:2555–62. doi:10.1016/j.proci.2014.05.068.

[31] Thrane C. Vacation motives and personal value systems. Journal of Vacation Marketing 1997;3:234–44. doi:10.1177/135676679700300305.

[32] Lindsay JD. The anisotropic permeability of paper: Theory, measurements, and analytical tools. IPC Technical Paper Series 1988;298.

[33] Segal L, Wakelyn PJ. Cotton fibres. Woodhead Publishing Limited; 1985. doi:10.1533/9780857095503.1.9.

[34] Chand N, Fahim MBT-T of NFPC, editors. Cotton reinforced polymer composites. Woodhead Publishing Series in Composites Science and Engineering, Woodhead Publishing; 2008, p. 129–61. doi:https://doi.org/10.1533/9781845695057.129.

[35] Wool M, Asbestos F. MINES BRANCH INVESTIGATION REPORT IR 73-42 n.d.

[36] Chawla KK. Fiber Fracture: An overview. In: Elices M, Llorca JBT-FF, editors. Fiber Fracture, Oxford: Elsevier Science Ltd; 2002, p. 3–25. doi:https://doi.org/10.1016/B978-008044104-7/50002-2.

[37] Zhao R, Sanjayan JG. Geopolymer and Portland cement concretes in simulated fire. Magazine of Concrete Research 2011;63:163–73. doi:10.1680/macr.9.00110.

[38] Mori K, Maki S, Tanaka Y. Warm and hot stamping of ultra high tensile strength steel sheets using resistance heating. CIRP Annals - Manufacturing Technology 2005;54:209–12. doi:10.1016/S0007-8506(07)60085-7.

[39] Costa A. Permeability-porosity relationship: A reexamination of the Kozeny-Carman equation based on a fractal pore-space geometry assumption. Geophysical Research Letters 2006;33:1–5. doi:10.1029/2005GL025134.

[40] Wang S, Huang X, Chen H, Liu N, Rein G. Ignition of low-density expandable polystyrene foam by a hot particle. Combustion and Flame 2015;162:4112–8. doi:10.1016/j.combustflame.2015.08.017.

[41] Xiong C, Huang X. Numerical Modeling of Flame Shedding and Extinction behind a Falling Thermoplastic Drip. Flow, Turbulence and Combustion 2021. doi:10.1007/s10494-021-00250-5.

[42] Xie Q, Zhang Z, Lin S, Qu Y, Huang X. Smoldering Fire of High-Density Cotton Bale Under Concurrent Wind. Fire Technology 2020;56:2241–56. doi:10.1007/s10694-020-00975-1.

[43] Quintiere JG. Fundamental of Fire Phenomena. New York: John Wiley; 2006.

doi:10.1002/0470091150.

[44] ASTM. Standard test method for measuring heat transfer rate using a thin-skin calorimeter. ASTM Standards 2005;05:1–11. doi:10.1520/D0882-12.2.

[45] Babrauskas V. Ignition Handbook. Issaquah, WA: Fire Science Publishers/Society of Fire Protection Engineers; 2003. doi:10.1023/B:FIRE.0000026981.83829.a5.

[46] Bergman TL, Lavine AS, Incropera FP, DeWitt DP. Fundamentals of heat and mass transfer, 2011. USA: John Wiley & Sons ISBN 2015;13:470–978.

Appendix

The dripping ignition is a complex process with large uncertainty. To reduce the experimental uncertainty, thousands of repeating tests were conducted, so that the dripping ignition probability can be quantified from Eq. (3). Fig. A1 plots the ignition probability of four papers under a fixing dripping frequency (1 Hz), and Fig. A2 plots the ignition probability under a fixed drip size (4.6 mg), where P_{ig} = 50% is defined as the critical dripping ignition limit [4], and these limiting curves are compared in Fig. 5.

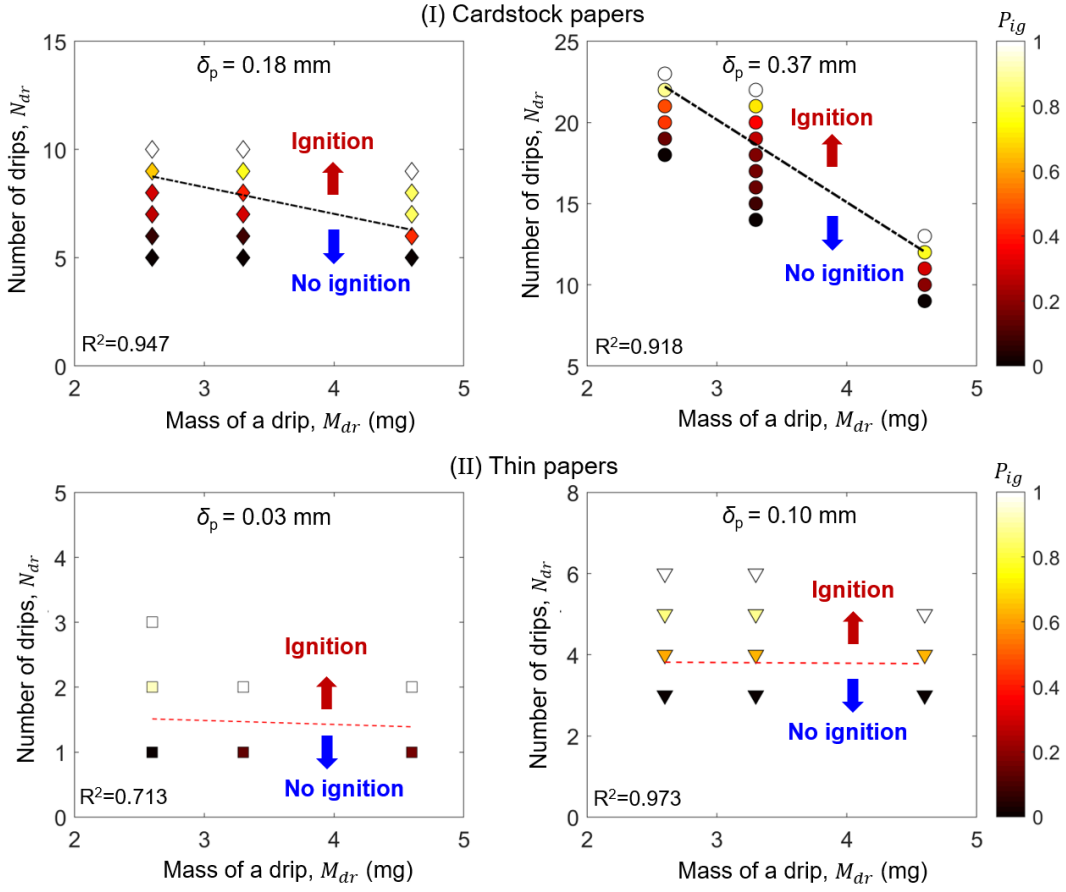

Fig. A1. The dripping ignition probability (P_{ig}) of four papers under the constant dripping frequency (1 Hz) and the varied drip size, where the critical dripping ignition condition is at P_{ig} = 50%.

With the varying drip size (or dripping frequency) and number of drips for ignition, the ignition probabilities are different, representing by the color of each point. The ignition limit is obtained by the linear regression. Above this limiting line, the ignition is happed. Below the line or below the minimum dripping frequency, no ignition would happen.

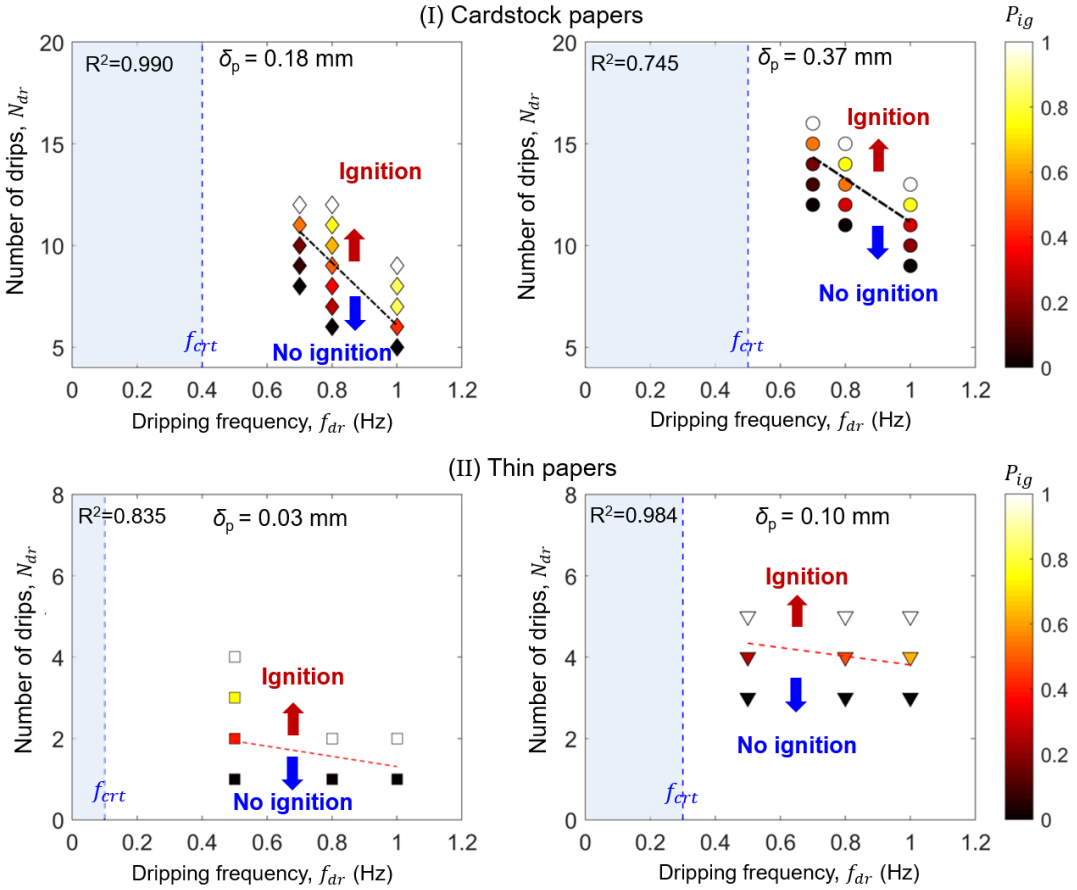

Fig. A2. The dripping ignition probability of four papers under the constant drip size (4.6 mg) and the varied dripping frequency.